DOI: 10.1002/cjoc.201300875

Highly Efficient Au/TiO_2 Catalyst for One-pot Conversion of Nitrobenzene to *p*-Aminophenol in Water Media

Luyao Zou, Yuanyuan Cui, and Weilin Dai*

Department of Chemistry and Shanghai Key Laboratory of Molecular Catalysis and Innovative Materials, *Fudan University*, *Shanghai 200433*, *China*

Au/TiO_2 catalyst is firstly reported to be efficient in the hydrogenation of nitrobenzene to produce *p*-aminophenol with a high PAP selectivity of 81% and overall yield more than 63%. The catalyst is also quite stable and can be reused for at least 4 times with only slight decrease in activity.

Keywords nitrobenzene, *p*-aminophenol, Au/TiO_2 catalyst, hydrogenation

Introduction

The Pd group metal catalysts[1-4] are widely used in the hydrogenation of nitroaromatics. The nitro group, through hydrogenation, is reduced to amine group, forming a series of corresponding aromatic amines of various utility. Compared with traditional Fe-concentrated HCl system, catalytic hydrogenation avoids complicated post-treatment and large amount of acidic sewage, thus is much more molecular economic and green.

Para-aminophenol (PAP) is an important raw material in synthesizing paracetamol,[5] the effective component in non-aspirin cold drug such as Tylenol®. The synthesis of PAP can be achieved by two hydrogenation pathways, the one is from paranitrophenol (PNP),[6-8] while the other is from nitrobenzene (NB) combined with a Bamberger rearrangement process.[9] For the latter one, a Brønsted acid is required for the rearrangement of *N*-phenylhydroxylamine (PHA), the intermediate of NB hydrogenation to aniline (AN) (see Scheme 1)[10]. Henke and Vaughen[11] showed that NB pathway is feasible using Pt/C catalyst in inorganic acid solution. Subsequent works improved the catalytic performance by optimizing reaction agents and conditions, pushing the selectivity of PAP up to 87% in sulfuric acid.[12] Meanwhile, corresponding kinetics was also carefully investigated, showing that hydrogenation rate is competitive against rearrangement rate, which limits the PAP selectivity even in concentrated acids.[13,14] Moreover, since NB is not soluble in water, the reaction happens in a four-phase system, *i.e.* gas, solid catalyst, aqueous and organic phases.[13] Although this property makes the separation of reagent and product easier (PAP and its sulphate are water soluble), it hinders the mass transfer process between molecules, and therefore the importation of phase-transfer agents may also improve the catalytic performance. Various solid acids have also been applied for this conversion for cleaner synthesis of PAP.[15-21] However, for metal-solid acid bifunctional catalysts, the high selectivity of PAP is more difficult to achieve. Most works could obtain a typically 50%—80% selectivity while the conversion of NB varies, but all made the overall yield of PAP less than 50%. Only Figueras *et al.*[20] reported the highest selectivity over 90% using the mechanical mixture of supported Pt and sulphated zirconia, but their reaction conditions varied and it was difficult for comparison. Recently, Liu *et al.*[22] reported a PAP yield of more than 47% using Pt/C catalyst and carbon-based solid acid.

The unique catalytic application of Au had not been realized until Haruta's work.[23] Compared with Pd group metals, Au is more inert in dissociating H—H bond, whereas more selective to certain functional groups in hydrogenation.[24] When catalyzing hydrogenation of *α*,*β*-unsaturated ketones, dinitroaromatic compounds and chlorinated aromatic compounds, unlike Pd group metals, Au will not cause the problems of hydrogenation of C=C dibond,[25] complete hydrogenation to diamine,[26] and dechlorination,[27] respectively. Chemoselective hydrogenation thus could be realized. Corma[28] and Bokhoven[29] proved that PHA is the main

Scheme 1 NB hydrogenation pathways

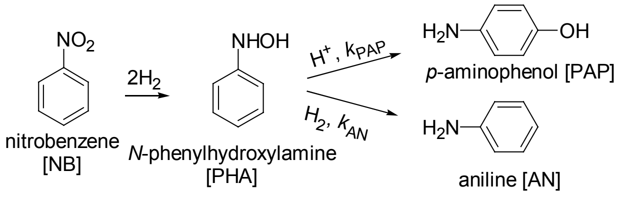

---

* E-mail: wldai@fudan.edu.cn

Received December 10, 2013; accepted January 22, 2014;

intermediate of NB hydrogenation on Au/TiO_2, and its hydrogenation to AN is the rate-determining step.[28] To our best knowledge, however, Au has not been reported in the direct conversion of NB to PAP. Whether Au could also have activity under strong acidic environment and could raise the selectivity in the conversion of NB to PAP, is a question yet to be answered.

Here we demonstrate that Au is also capable of catalysing NB hydrogenation in sulfuric acid, with a high PAP selectivity of 81% in pure aqueous media without any phase-transfer agents, and with much lower acid concentration requirement than reported Pd or Pt catalysts. Among various investigated supports (TiO_2 (P25), ZrO_2[30], CeO_2[31]) and acids (H_2SO_4, TsOH, $H_3PW_{12}O_{40}$), P25 and H_2SO_4 showed the best match with Au.

Experimental

Catalyst preparation

Gold was supported on commercial TiO_2 (Degussa). A traditional deposition-precipitation (DP) method first introduced by Haruta[23] was applied. First, 0.2 mol•L^{-1} NaOH was used to adjust the pH of 100 mL $HAuCl_4$ (0.51 mmol•L^{-1}) precursor to 7.2, then a certain amount of P25 was dispersed in the solution under continuous magnetic stirring to get the 1 wt% loading. The dispersion was heated to 333 K in complete darkness for 2 h with stirring, then it was cooled to room temperature and filtered. The as-prepared catalyst was washed with deionized water until no Cl^- was detected in the filtrate by $AgNO_3$, then dried in air at 353 K overnight and calcined in air at 573 K for 2 h with a heating rate of 2 K•min^{-1}.

Other supports such as ZrO_2, CeO_2, SO_4^{2-}/ZrO_2 and ZSM-5 were prepared according to previous reports.[30,31] Briefly, ZrO_2 was prepared by refluxing $Zr(OH)_2$ precipitated from $ZrOCl_2$ in ammonia at 373 K for 40 h before calcinations. CeO_2 was prepared by hydrothermal method. SO_4^{2-}/ZrO_2 was prepared by impregnating refluxed $Zr(OH)_2$ in dilute H_2SO_4 solution before calcination.

Catalytic activity measurement

Reaction was performed in an autoclave with approximately 90 mL volume. Typically, 0.3 g NB, 50 mg catalyst, 10 mL sulfuric acid, 1 MPa H_2, 4 h and stirring rate of 800 r/min were chosen. Acid concentration and reaction temperature were investigated. Products were analyzed by HPLC with methanol-water solution (V/V 4∶6). The composition of the buffer is 4 mmol•L^{-1} NaH_2PO_4 and 8 mmol•L^{-1} Na_2HPO_4. Peaks other than NB, AN and PAP were weak enough to be ignored, and PHA was not detectable. The performance of the catalyst was measured by the conversion of NB and selectivity of PAP and AN by using the typical calculating method:

$$\text{Conv.(NB)}=\left(1-\frac{f_{\text{NB}}(A_{\text{NB}})}{\sum_i f_i(A_i)}\right)\times 100\%$$

$$\text{Sel.(PAP)}=\frac{f_{\text{PAP}}(A_{\text{PAP}})}{\sum_i f_i(A_i)}\times 100\%$$

$$\text{Sel.(AN)}=\frac{f_{\text{AN}}(A_{\text{AN}})}{\sum_i f_i(A_i)}\times 100\%$$

where A_i represents the peak area of each component, and $c_i=f_i(A_i)$ is the mole concentration calculated from the peak area according to the standard curves. Assume that all Au nanoparticles are semi-sphere on the support and half area of surface Au atoms is exposed, TOF is calculated according to the following equations:

$$\text{disp}=\frac{\text{number of surface Au atoms}}{\text{number of all Au atoms}}=\frac{3M_{\text{r}}\times\alpha}{D\times\rho\times N_{\text{A}}}$$

$$N_{[\text{surf Au atoms}]}=\frac{m_{[\text{catal}]}}{M_{[\text{Au}]}}LN_{\text{A}}\bullet\text{disp}$$

$$\text{TOF}=\frac{N_{[\text{NB converted}]}}{tN_{[\text{surf Au atoms}]}}$$

where D is the average diameter of Au nanoparticles, $a=1.15\times10^{19}/\text{m}^2$ is the surface atomic concentration constant of Au, ρ is the density of Au, L is Au loading, N_A is Avogadro constant.

Characterization

The Au loading of the catalysts was measured by inductively coupled plasma atomic emission spectroscopy (ICP-AES) using a Hitachi P-4010 ICP spectrometer. Samples were first dispersed in aqua regia in order to dissolve all Au, and then sent for analysis. XRD patterns of the samples were recorded on a Bruker D8 advance diffractometer with Cu Kα radiation ($\lambda=0.154$ nm), operated at 40 mA and 40 kV. The scanning rate was 4 (°)•min^{-1} from 20° to 85°. N_2 adsorption profiles of the samples were performed in Micromeritics Tristar ASAP 3000 at 77 K. Specific surface areas of the samples were calculated by using Brunauer-Emmett-Teller (BET) method. TEM images of the catalysts were taken by a JEOL 2011 electron microscope operating at 200 kV. Samples were first dispersed in ethanol and deposited onto a carbon-coated copper grid before being moved into the TEM vacuum chamber. The average size and size distribution of the Au nanoparticles were determined by measuring more than 150 Au particles on the images. XPS analysis was performed using a Perkin Elmer PHI 5000C ESCA system equipped with a hemispherical electron energy analyzer. The Mg Kα ($hv=$ 1253.6 eV) anode was operated at 14 kV and 20 mA.

The energy scale was internally calibrated by setting the C_{1s} peak at 284.6 eV.

Results and Discussion

Comparing various support, we found that Au/ZrO_2 was less active than Au/TiO_2 in our experiment, and CeO_2 was not stable enough even in dilute H_2SO_4. For solid acids, mechanical mixture was not able to carry out the rearrangement reaction, and Au was also difficult to be supported because of the strongly acidic surface. Therefore, Au/TiO_2 was eventually chosen as the ideal catalyst.

BET analysis shows that the surface areas before (51.0 $m^2 \cdot g^{-1}$) and after (50.2 $m^2 \cdot g^{-1}$) 1% Au loading have no significant change, indicating that the surface structure of the support is not effected by Au nanoparticles. The pH condition and calcination temperature were both optimized to obtain well-dispersed Au nanoparticles of best catalytic performance. It is consistent with other reported works that pH determines the loading and dispersion of $Au(OH)_3$ species and further Au particle size on the surface of TiO_2.[32]

A series of Au/TiO_2 catalysts with Au loading ranging from 1% to 3% were prepared. Physicochemical properties of the catalysts and their reaction performance are summarized in Table 1. XRD patterns (Figure 1) show no distinguishable difference between catalysts of different Au loading. All of the patterns correspond to anatase-rutile mixed phase of TiO_2, without diffraction peaks of Au detected which is due to the low loading of Au and its ultra-small particle size. XPS characterization (Figure 2) identifies the surface chemical state of Au species. Although calcined in air, there was almost completely metallic Au found on the surface. Catalysts of different Au loading showed only the difference in XPS peak areas, while the binding energy remained nearly the same. This finding means the uniformity of surface state remains while Au loading varies. The exact Au loading was determined by ICP as 0.89%, 1.55% and 1.84%, respectively. The Au content deviated from the theoretical values at high Au loading, indicating the difficulty in loading large amount of Au onto the support. From the TEM images (see Figure 3), we found that 1% Au/TiO_2 gives the smallest average particle size. Although it is well accepted that Au nanoparticles with small particle size should show high catalytic activity,[33] TOF calculation shows that the difference is moderate between the catalysts when the reaction rate is normalized to per surface Au unit, discounting the effect of catalyst loading. This may imply that the catalytic activity is not so sensitive to the particle size when the mean particle size is below 5 nm. Nevertheless, 1% Au/TiO_2 still owns the best dispersion and economic efficiency, therefore 1% was chosen as the typical Au loading amount.

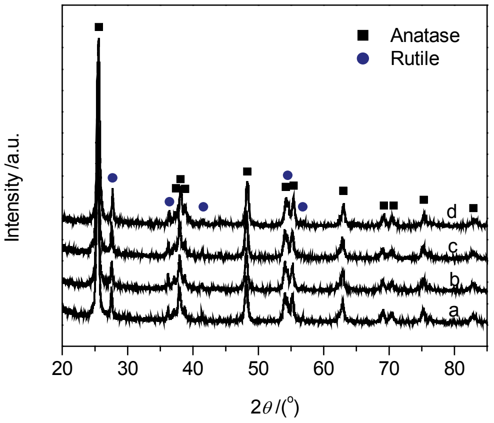

Figure 1 XRD patterns of (a) TiO_2; (b) 1% Au/TiO_2; (c) 2% Au/TiO_2; (d) 3% Au/TiO_2.

A series concentration of H_2SO_4 from 0 to 1.0 $mol \cdot L^{-1}$ was applied to investigate the effect of acid concentration on PAP selectivity. Figure 4 shows that if pure water (*i.e.* $c(H_2SO_4)=0$) was used, the main product was AN and there was no PAP detected, proving the necessity of acid in the rearrangement. HPLC peaks of the amount of by-products other than NB, AN and PAP were too low to be detected. The drop on NB conversion may be ascribed to the aggregation of Au nanoparticles on the surface, since we observed the particle size growth after reaction. To our surprise, selectivity results were greatly different from those of Pt and Pd catalysts reported by other works.[10,12,13] We found when $c(H_2SO_4)$ was larger than 0.1 $mol \cdot L^{-1}$, the selectivity of PAP kept quite stable at about 81% with a fluctuation within 5%, which is within normal experimental error. Usually for Pt and Pd catalysts, the maximum selectivity of PAP could only be achieved at comparatively high acid concentration (5—10 wt% for example), and both lower and higher concentration could cause the decrease

Table 1 Physicochemical properties and performance of Au/TiO_2 catalysts with Au loading of 1%, 2% and 3%[a]

Catalyst Au/TiO_2	Au loading[b]/wt%	Surface Au/Ti ratio ($\times 10^{-2}$)[c]	Mean particle size/nm	Au $4f_{7/2}$ binding energy/eV	Conv./%	Sel./% PAP	Sel./% AN	TOF[d]/h^{-1}
1%	0.89	1.35	2.5	83.0	78	81	19	914
2%	1.55	1.23	2.9	82.8	41	86	14	923
3%	1.84	2.08	4.6	82.8	34	83	17	1137

[a] Reaction conditions: 0.3 g NB, Au/TiO_2=50 mg (1%), 25 mg (2%), 17 mg (3%), 10 mL H_2SO_4, 373 K, 1 MPa H_2, 4 h and 800 r/min. [b] Analyzed by ICP. [c] Calculated according to XPS peak areas. [d] Attributed to initial conversion rate of NB molecules per surface Au atom per second.

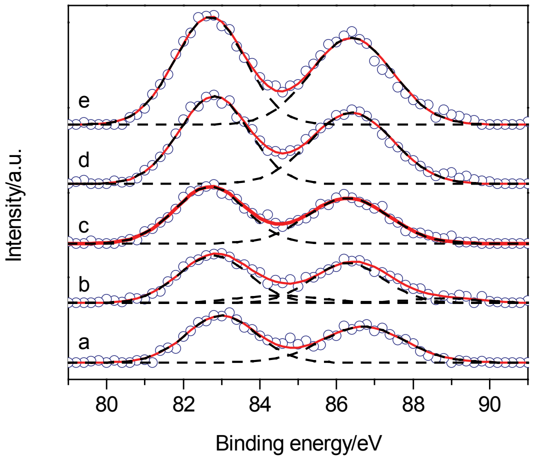

Figure 2 XPS spectra of (a) 1% Au/TiO_2; (b) 1% Au/TiO_2 after reaction without calcination; (c) 1% Au/ TiO_2 after re-calcination; (d) 2% Au/ TiO_2; (e) 3% Au/ TiO_2.

in PAP selectivity. In our own comparison experiment at 0.1 mol•L^{-1} H_2SO_4 using 5% Pd/C purchased from UChem Co. Ltd., NB was completely converted within 30 min but PAP selectivity was below 25%. This phenomenon indicates that when Au is used in this reaction system, the hydrogenation rate of PHA intermediate is much slower than the rearrangement rate. This result is probably due to the weak dissociation ability of Au to H—H bond. Although it is a weakness in other situations, the property here is rather an advantage to weaken the comparative hydrogenation of PHA to AN by-product.

The results of different reaction temperatures on the reaction are shown in Figure 5. The conversion of NB increases with the temperature, while the selectivity to PAP first increases and then drops obviously. The maximum selectivity of PAP is achieved at 363 K. Because of the complexity of the four-phase reaction, it is difficult to determine the mechanism of each intermediate step. Nevertheless, according to the previous research, the selectivity to PAP is determined by the reaction rate ratio of rearrangement and hydrogenation of PHA, k_{PAP}/k_{AN}.[20] When T rises, the hydrogenation rate of both NB and PHA increases faster than the rearrangement rate of PHA, resulting in the increase of NB conversion as well as AN yield, which corresponds well to the right-hand side of Figure 5. Considering the left-hand side is against the reasons above, we also assume that there is also a chemical desorption process. As we know, H_2 and NB are adsorbed on the surface of Au, and Bokhoven *et al.* also observed PHA adsorption only on Au-TiO_2 interface.[34-36] Therefore, the hydrogenation of NB and PHA occurred on the surface. On the other hand, H^+ is in the bulk solution, so PHA may first desorb from the surface before its rearrangement (see Figure 6). It can be expected that the desorption rate also accelerates while the reaction temperature increases. At low temperature, a limited desorption rate restrains the rearrangement in the bulk, leading to lower PAP selectivity. To investigate the reusability of the

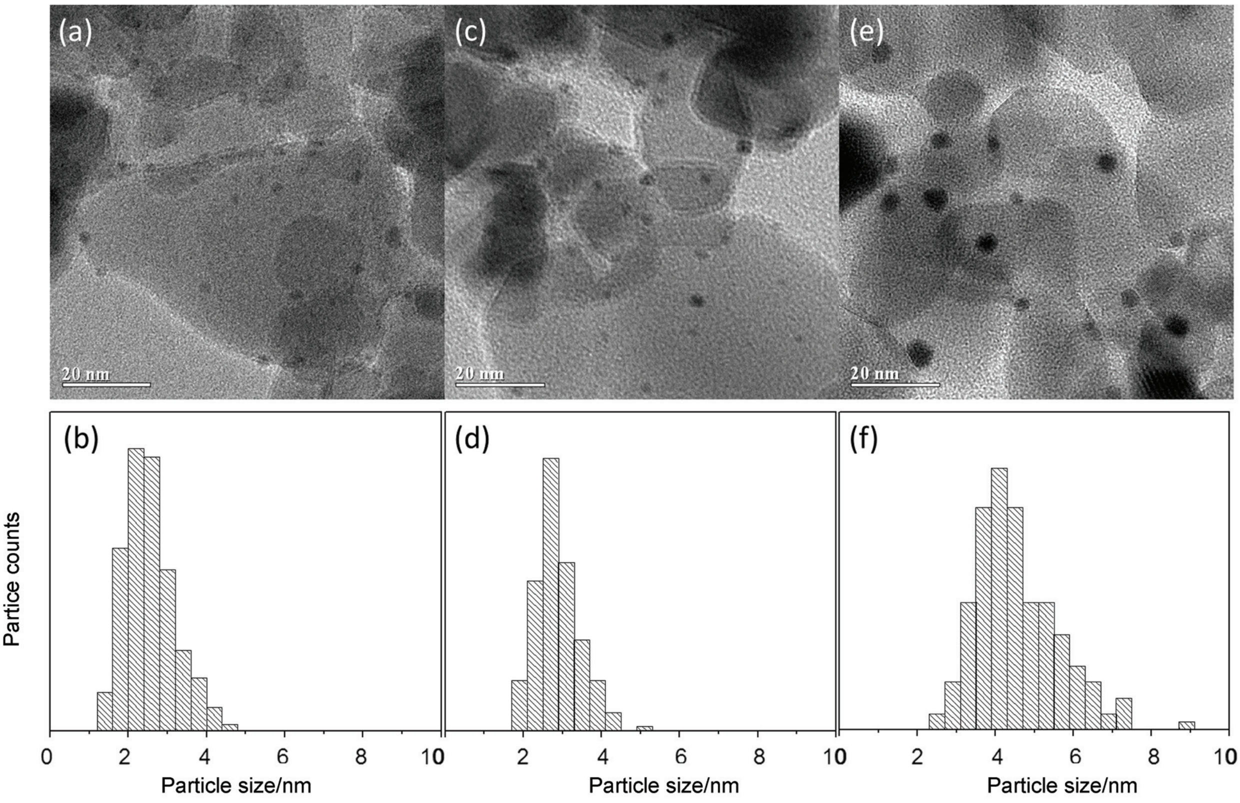

Figure 3 TEM images of (a, b) 1% Au/TiO_2; (c, d) 2% Au/ TiO_2; (e, f) 3% Au/TiO_2 and particle size distribution of Au.

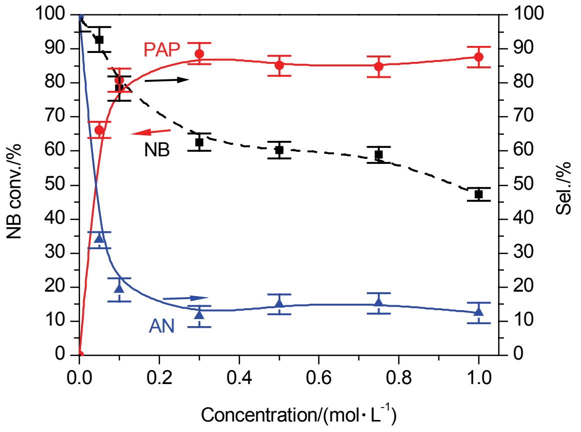

Figure 4 NB conversion and PAP, AN selectivity at different H_2SO_4 concentration. Reaction conditions: 0.3 g NB, 50 mg catal., 10 mL H_2SO_4, 373 K, 1.0 MPa H_2, 4 h and 800 r/min.

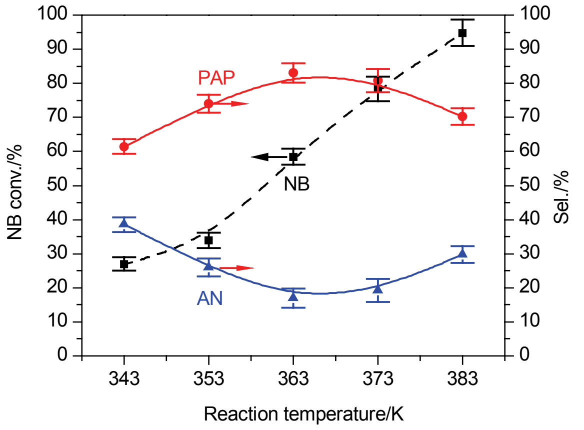

Figure 5 NB conversion and PAP, AN selectivity at different reaction temperature. Reaction conditions: 0.3 g NB, 50 mg catal., 10 mL 0.1 mol•L^{-1} H_2SO_4, 1.0 MPa H_2, 4 h and 800 r/min.

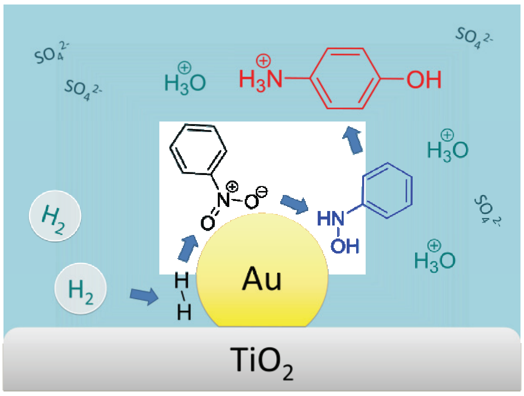

Figure 6 Probable mechanism of the hydrogenation, desorption and rearrangement.

catalyst, after reaction, the catalyst was collected by centrifugation and washed with methanol, and then dried and calcined at 573 K for 2 h (ramping rate, 2 K•min^{-1}). Then it was reused for the next run, while the amount of NB was stoichiometrically adjusted according to the exact weight of the catalyst added. Meanwhile, another sample without calcination was also collected for comparison. A considerable activity loss of the non-calcined catalyst was observed at the second run, as NB conversion dropped to only 35%. The selectivity to PAP slightly increased to 90%, maybe due to a slower hydrogenation rate of PHA. However, after calcination, the catalyst was recovered to show 80% NB conversion and 84% PAP selectivity (see Figure 7). XPS analysis reveals that after the reaction, a small amount of ositive Au species appear (see Figure 2), whose 4f 7/2 binding energy locates at 84.5 eV. The small peak disappears again after the calcinations process. This finding may imply the significance of calcination in re-activating the spent catalyst.

After the fourth run, a slight decrease in NB conversion was observed, indicating the good stability of Au/TiO$_2$ catalyst in the title reaction.

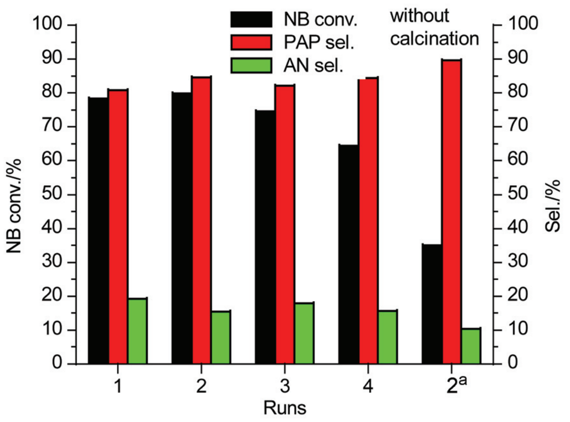

Figure 7 Repeat use of 1% Au/TiO$_2$. 2^a: Second-run with non-calcined catalyst. Reaction conditions: *m*(NB) : *m*(catal.)= 6 : 1, 10 mL 0.1 mol•L^{-1} H_2SO_4, 1.0 MPa H_2, 4 h and 800 r/min.

Conclusions

In summary, we have successfully applied Au/TiO$_2$ catalyst in the hydrogenation of NB to PAP for the first time. The catalyst shows superior activity in water media with high NB conversion (78%) and PAP selectivity (81%), and is quite stable in repeated usage for at least 4 runs. Future research will be focused on the design of an effective synthesis route with highly dispersed Au species on acidic support in order to get multi-functional catalyst.

Acknowledgement

Financial support by the Major State Basic Resource Development Program (Grant No. 2012CB224804), NSFC (Project Nos. 21373054, 21173052), the Natural Science Foundation of Shanghai Science and Technology Committee (No. 08DZ2270500) and Hui-Chun Chin and Tsung-Dao Lee Chinese Undergraduate Research Endowment (CURE).

References

[1] Downing, R.; Kunkeler, P.; van Bekkum, H. *Catal. Today* **1997**, *37*, 121.

[2] Lu, P.; Teranishi, T.; Asakura, K.; Miyake, M.; Toshima, N. *J. Phys. Chem. B* **1999**, *103*, 9673.

[3] Liang, M.; Wang, X.; Liu, H.; Liu, H.; Wang, Y. *J. Catal.* **2008**, *255*, 335.

[4] Mahata, N.; Cunha, A.; Órfãoand, J. J. M.; Figueiredo, J. *Catal. Commun.* **2009**, *10*, 1203.

[5] Osborne, C. *Paracetamol*: *A Curriculum Resource*, Royal Society of Chemistry, Cambridge, UK, **2002**, p. 24.

[6] Du, Y.; Chen, H.; Chen, R.; Xu, N. *Appl. Catal. A*: *Gen.* **2004**, *277*, 259.

[7] Lu, H.; Yin, H.; Liu, Y.; Jiang, T.; Yu, L. *Catal. Commun.* **2008**, *10*, 313.

[8] Wang, A.; Yin, H.; Ren, M.; Lu, H.; Xue, J.; Jiang, T. *New J. Chem.* **2010**, *34*, 708.

[9] Bamberger, E. *Berichte Der Deutschen Chemischen Gesellschaft* **1894**, *27*, 1548.

[10] Rode, C. V.; Vaidya, M. J.; Chaudhari, R. V. *Org. Process Res. Dev.* **1999**, *3*, 465.

[11] Henke, C. O.; Vaughen, J. V. *U.S. Patent 2198249*, **1940**.

[12] Tanielyan, S. K.; Nair, J. J.; Marin, N.; Alvez, G.; McNair, R. J.; Wangand, D.; Augustine, R. L. *Org. Process Res. Dev.* **2007**, *11*, 681.

[13] Rode, C.; Vaidya, M.; Jaganathan, R.; Chaudhari, R. *Chem. Eng. Sci.* **2001**, *56*, 1299.

[14] Nadgeri, J. M.; Biradar, N. S.; Patil, P. B.; Jadkar, S. T.; Garade, A. C.; Rode, C. V. *Ind. Eng. Chem. Res.* **2011**, *50*, 5478.

[15] Gao, Y.; Wang, F.; Liao, S.; Yu, D. *React. Kinet. Catal. Lett.* **1998**, *64*, 351.

[16] Komatsu, T.; Hirose, T. *Appl. Catal. A*: *Gen.* **2004**, *276*, 95.

[17] Ratnam, K. J.; Reddy, R. S.; Sekhar, N.; Kantam, M. L.; Deshpande, A.; Figueras, F. *Appl. Catal. A*: *Gen.* **2008**, *348*, 26.

[18] Wang, S.; Ma, Y.; Wang, Y.; Xue, W.; Zhao, X. *J. Chem. Technol. Biotechnol.* **2008**, *83*, 1466.

[19] Liu, P.; Hu, Y.; Ni, M.; You, K.; Luo, H. *Catal. Lett.* **2010**, *140*, 65.

[20] Deshpande, A.; Figueras, F.; Kantam, M. L.; Ratnam, K. J.; Reddy, R. S.; Sekhar, N. *J. Catal.* **2010**, *275*, 250.

[21] Wang, S.; He, B.; Wang, Y.; Zhao, X. *Catal. Commun.* **2012**, *24*, 109.

[22] Liu, Y. X.; Fang, Y. Y.; Lu, X. L.; Wei, Z. J.; Li, X. N. *Chem. Eng. J.* **2013**, *229*, 105.

[23] Haruta, M.; Yamada, N.; Kobayashi, T.; Iijima, S. *J. Catal.* **1989**, *115*, 301.

[24] Corma, A.; Serna, P. *Science* **2006**, *313*, 332.

[25] He, L.; Yu, F. J.; Lou, X. B.; Cao, Y.; He, H. Y.; Fan, K. N. *Chem. Commun.* **2010**, *46*, 1553.

[26] Cárdenas-Lizana, F.; Gómez-Quero, S.; Keane, M. *Catal. Lett.* **2009**, *127*, 25.

[27] He, D.; Shi, H.; Wu, Y.; Xu, B. Q. *Green Chem.* **2007**, *9*, 849.

[28] Corma, A.; Concepción, P.; Serna, P. *Angew. Chem.*, *Int. Ed.* **2007**, *46*, 7266.

[29] Makosch, M.; Sá, J.; Kartusch, C.; Richner, G.; van Bokhoven, J. A.; Hungerbühler, K. *ChemCatChem* **2012**, *4*, 59.

[30] Jung, K. T.; Bell, A. T. *J. Mol. Catal. A*: *Chem.* **2000**, *163*, 27.

[31] Mai, H. X.; Sun, L. D.; Zhang, Y. W.; Si, R.; Feng, W.; Zhang, H. P.; Liu, H. C.; Yan, C. H. *J. Phys. Chem. B* **2005**, *109*, 24380.

[32] Wolf, A.; Schuth, F. *Appl. Catal. A: Gen.* **2002**, *226*, 1.

[33] Cárdenas-Lizana, F.; Gómez-Quero, S.; Idriss, H.; Keane, M. A. *J. Catal.* **2009**, *268*, 223.

[34] Claus, P. *Appl. Catal. A*: *Gen.* **2005**, *291*, 222.

[35] Boronat, M.; Concepción, P.; Corma, A.; González, S.; Illas, F.; Serna, P. *J. Am. Chem. Soc.* **2007**, *129*, 16230.

[36] Richner, G.; van Bokhoven, J. A.; Neuhold, Y. M.; Makosch, M.; Hungerbühler, K. *Phys. Chem. Chem. Phys.* **2011**, *13*, 12463.

(Pan, B.; Qin, X.)